Compression and caging of CD_3Cl by H_2O layers on Ru(001)

Y. Lilach and M. Asscher
Department of Physical Chemistry and the Farkas Center for Light Induced Processes, The Hebrew University, Jerusalem 91904, Israel

(Received 15 February 2002; accepted 17 July 2002)

The interaction of two similar coadsorbed dipolar molecules H_2O and CD_3Cl has been studied as a function of coverage over Ru(001) under ultra high vacuum conditions. The complementary techniques of temperature-programmed desorption mass spectrometry (ΔP-TPD) and work function change in a $\Delta\phi$-TPD mode were employed. Adsorption of water on top of CD_3Cl reveals two major trends: At submonolayer methyl chloride coverage, post-deposited water compresses the methyl chloride molecules and forces them to flip over to the methyl down configuration at the second layer, leading eventually to three-dimensional islands. This is indicated by both CD_3Cl ΔP-TPD and differential work function $[d(\Delta\phi)/dT]$ data. Higher water coverage $[\theta(H_2O) > 1.2$ bilayers (BL)] causes full detachment of the CD_3Cl molecules from the ruthenium surface, to be encapsulated within the amorphous solid water (ASW) layer that is formed. At even higher water coverage $[\theta(H_2O) > 5$ BL], methyl chloride desorbs in an explosivelike mode at 165 K. The caged methyl chloride molecules lack any permanent dipole moment as indicated from differential $\Delta\phi$-TPD analysis, explained in terms of a high level of disorder within the ASW. The relevance of the hydrophobic caging process to clathrate-hydrate formation is discussed. © *2002 American Institute of Physics.* [DOI: 10.1063/1.1505858]

I. INTRODUCTION

Electrostatic interactions among coadsorbates on solid surfaces are of great importance at moderate to high surface coverages, conditions that often exist in realistic industrial catalytic processes. Dipole–dipole interactions between neighbor adsorbates were considered in the literature for several model systems, such as alkali metals[1–3] and alkyl halides,[4–6] in order to explain their unique temperature-programmed desorption (TPD) and work function change spectra, as a function of coverage. In most of these cases, repulsion is the dominant feature as coverage increases, leading to a significant decrease in the desorption temperature. In many of these systems this is associated with a concomitant decrease in the work function, e.g., for alkali metals and alkyl halides on transition metals. When large dipoles are close enough to each other at high coverages, depolarization effects that tend to decrease the effective dipole moments need to be accounted for.[3]

On the basis of this introduction a particularly interesting pair of dipoles to compare and interact is that of methyl chloride and water molecules. Both have identical dipoles of 1.89 D in the gas phase, and both change to similar dipoles upon adsorption on metal surfaces [on Ru(001) the measured dipole is 2.2 D (Refs. 6 and 8)]. While having identical dipoles, they display an opposite type of interaction on metallic surfaces: methyl chloride molecules repel each other, while the water molecules strongly attract each other.[7] The attraction arises from the unique hydrogen bonding that occurs among neighbor adsorbed water molecules, thus overcoming the repulsion due to similar and possibly parallel dipoles.

The interaction between such molecules that behave in an opposite manner cannot be predicted on the basis of the behavior of each separately. The goal of the study to be presented below is to explore the unique outcome of strong electrostatic interactions among repelling (CD_3Cl) and attracting (H_2O) molecules on a smooth metallic surface—Ru(001), on which the interaction of the separate molecules have been studied extensively.[6–8,16,17] In one instance, this combination of molecules has been studied on top of Cu(110),[9] with the sole interest, however, in the adsorption properties and characteristics of CH_3Cl on top of preadsorbed water. A different study used D_2O layers as spacers between a Pt(111) surface and layers of CH_3Cl to understand the behavior of the photochemical cross section.[10] As will be demonstrated below, the opposite adsorption order—namely, methyl chloride first and then water—enables us to explore a whole new type of phenomena that originate from the strongly repelling dipoles.

The first observation of the formation of cages of coadsorbates under water layers on metallic surfaces was that of N_2 molecules on Ru(001). This study was reported by Livneh *et al.*,[11] who studied this system utilizing complementary TPD and work function change measurements. An explosive desorption peak of N_2 displaying a width of 2 K has been observed near 165 K, at the onset of the ice layer desorption.[11] In a subsequent study Smith *et al.*[12] observed a similar behavior in the case of CCl_4 under a thicker layer of ice over Au(111) and Ru(001) surfaces. They have interpreted this explosive desorption as a ''volcano''-like behavior that originates from the onset of crystallization of the amorphous solid water layer to ice near 165 K. Similar behavior has recently been observed also when oxygen was trapped under water over TiO_2 surface.[13]

In this report we utilize a combination of ΔP-TPD (the

typical thermal desorption mass-spectrometry mode) with $\Delta\phi$-TPD, where the work function change is monitored while adsorption takes place and then during the temperature ramp used in normal TPD. The combination of these two techniques provides a unique ability to monitor structural changes made by adsorbed molecules *before* and *during* their desorption and thus provides deeper insight into the structure and stability of the adsorbed molecules.[6,14] The current study focuses on the interaction between two strong dipoles that form a cage, unlike the previous reports,[11–13] where nondipolar molecules were trapped inside the cage, and therefore their packing process and rearrangement could not be monitored.

II. EXPERIMENT

The experiments were performed in a UHV chamber, described previously,[6] with a base pressure of 2×10^{-10} Torr. Briefly, a Ru(001) sample [oriented within $\pm0.1°$ off the (001) crystal orientation] was mounted to two Ta legs, attached to a liquid nitrogen reservoir. The sample could be cooled down to 82 K by pumping over the reservoir and was resistively heated via 0.5-mm Ta wires spot-welded to the sample edges. Work function change measurements ($\Delta\phi$) were performed using a Kelvin probe (Besocke, Kelvin probe type S), attached to a translation stage, with its gold reference electrode shielded against sputter and other evaporation impurities. An ac-current heating scheme enables $\Delta\phi$ measurement and sample heating simultaneously, to obtain $\Delta\phi$-TPD spectra with a typical resolution of 2 meV. These spectra were recorded by a LABVIEW computer program, which also generated the spectra to obtain the $d(\Delta\phi)/dT$ plots presented below. ΔP-TPD were measured by monitoring simultaneously masses 53 and 14 for CD_3Cl and mass 17 for H_2O (the signal at mass 18 cannot be utilized because of the CD_3 signal background at this mass, obtained from CD_3Cl fragmentation at the ionizer). The heating rate in all TPD measurements was 2 K/sec.

CD_3Cl and triple-distilled H_2O were introduced into the chamber via standard leak valves backfilling the chamber. CD_3Cl of 99.5% purity was further cleaned by a few freeze-pump-thaw cycles. It was monitored regularly by measuring its mass spectra to follow possible H/D exchange in the gas introduction lines.

III. RESULTS AND DISCUSSION

A. CD_3Cl and H_2O separately on Ru(001)

1. CD_3Cl on clean Ru(001)

CD_3Cl adsorbs molecularly on Ru(001) at 82 K and desorbs intact at all coverage ranges, as indicated from the lack of any deuterium desorption. Exposure of 4.5 L CD_3Cl (corrected for ion gauge sensitivity) leads to four distinct Δp-TPD peaks [Fig. 1(a)]. These peaks are associated with three layers of CD_3Cl and one unsaturable multilayer. The first layer adsorption is dominated by strong repulsive dipole–dipole interactions and depolarization effects,[6] resulting in a broad TPD peak which stretches between 220 and 150 K. $\Delta\phi$ measurement during adsorption [Fig. 1(b)] shows a *decrease* of -2.04 eV in the work function at the completion of the first layer. This suggests that the first layer is adsorbed with the chlorine facing the metal surface. At higher coverages a second TPD peak emerges at 140 K, which does not broaden upon further coverage increase. In this coverage range the work function *increases* ($\Delta\phi = 0.4$ eV), explained by a flipped adsorption geometry, on average, of most of the second layer molecules, with the chlorine facing up, as discussed below. This flipped-layer structure resembles the packing in crystalline methyl halides.[15]

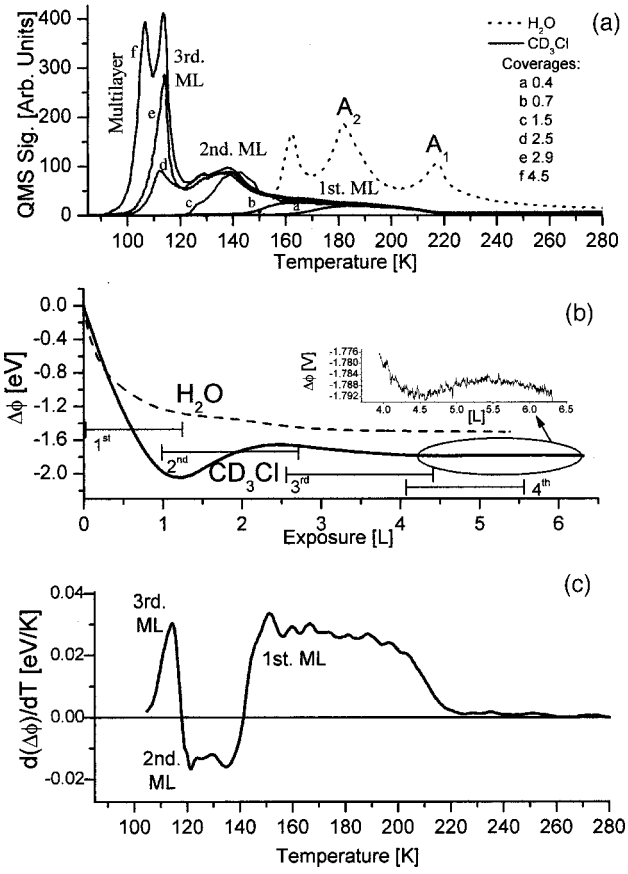

FIG. 1. (a) ΔP-TPD of CD_3Cl at 53 amu (solid line) and H_2O (dashed line) from a clean Ru(001) surface. CD_3Cl coverages are from 0.4 to 4.5 ML, as indicated. Water coverage is 1.3 BL. Heating rate was 2 K/sec throughout. (b) Work function change during adsorption of CD_3Cl (solid line) and H_2O (dashed line) on a clean Ru(001) surface. The inset is an expansion of the section between 4 and 6.5 L. The exposure range that results defines each of the first layers is marked. $\Delta\phi<0$ in the first and third layers, while in the second and fourth layers $\Delta\phi>0$. (c) $d(\Delta\phi)/dT$ of CD_3Cl on a clean Ru(001) surface obtained from the $\Delta\phi$-TPD spectrum, initially at a coverage of 3 ML.

A turnover and increase of the work function at a certain coverage, as seen in Fig. 1, resembles the work function change of alkali metals.[2,3] However, there is a major difference between these two systems regarding the physical origin of this phenomenon. In the case of the alkali metals, the turnover occurs at a coverage near 0.5 ML, as a result of a gradual change from single ionic metal adsorbates to neutral clusters,[3(b)] which also affects the polarizability of the adsorbed species.[3(c)] It was shown that this turn over cannot be explained on the basis of depolarization only.[3(a)]

The methyl chloride case is different. The actual charge

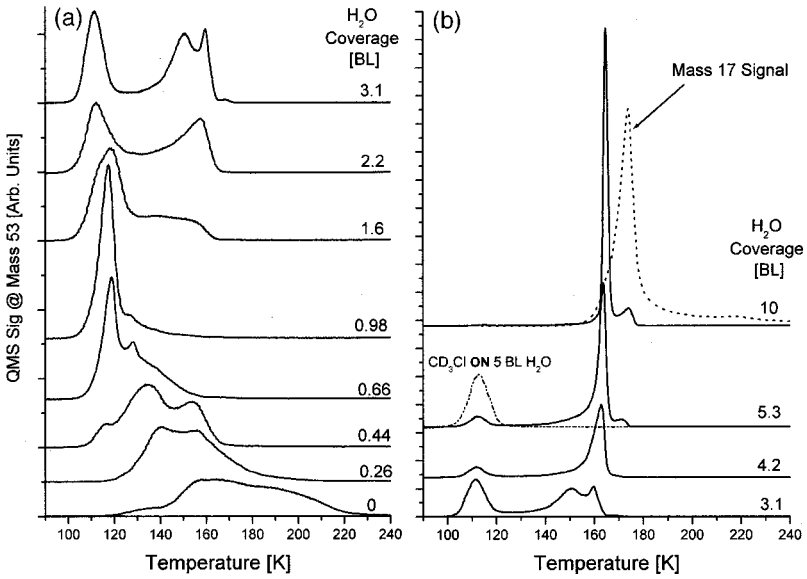

FIG. 2. ΔP-TPD at 53 amu (CD_3Cl) following water post-deposition. Water coverage is indicated in bilayers (BL) on top of a fixed CD_3Cl coverage of 0.7 ML. The dash-dotted line [in (b)] is ΔP-TPD spectrum of the reversed adsorption order—0.7 ML CD_3Cl *on top* of 5.3 BL of water.

and permanent dipole of the molecule are not expected to change significantly with coverage. Moreover, the coverage where the turnover takes place in the case of methyl chloride has been very carefully determined to be at the completion of the first monolayer.[6,14] The only explanation, therefore, for the turnover of the slope of the work function change with coverage in this case is that most of the second-layer molecules flip to the methyl down configuration upon adsorption at 82 K.

We assume that the size of the dipole moment of the methyl chloride molecules (μ) in each of the layers is fixed (ignoring minimal depolarization effects and image charge). Under these conditions we may estimate a lower limit for the fraction of molecules in the second layer that are oriented with their chlorine atom up, on average. The work function change is given by $\Delta\phi = 4\Pi\mu n$, with n the density of surface molecules. $|\Delta\phi|$ for the first layer is 2.04 and 0.4 eV for the second [Fig. 1(b)]. This leads to a ratio $n_2/n_1 = 0.4/2.04 = 0.19$, where $n_{1,2}$ are the densities in each of the first two layers. In the extreme case of only vertically oriented molecules (pointing either straight up or down), that means that an excess (lower limit value) of 19% of a monolayer of CD_3Cl molecules are aligned with their chlorine up in the second layer. A more realistic description of the layer, with varying molecular orientations, should result in a larger excess of the chlorine up molecules.

Adsorption of the third layer (observed in TPD as a sharp peak at 114 K) is accompanied again by a small *decrease* in the work function. Finally, an unsaturable multilayer peak appears at 108 K. The inset in Fig. 1(b) reveals that molecules at the third and fourth layers are again on average flipped over with respect to each other, but at diminishing excess. The lower limit for excess molecules that are oriented as discussed above is 6% at the third layer and a very small excess at the fourth layer [still resolved experimentally, as seen in the inset of Fig. 1(b)] to molecules that are oriented with the chlorine up. The alternating orientation structure is clearly demonstrated by the $d(\Delta\phi)/dT$ spectrum shown in Fig. 1(c), where the opposite work function change is depicted for each of the desorbing layers. This indicates that no significant restructuring takes place within the adsorbed methyl chloride molecules during the temperature ramp in TPD [Fig. 1(c)] and the molecules are packed structurally similar to their state during adsorption at 82 K [Fig. 1(b)].

We thus conclude that the reason for the diminishing magnitude of the alternating work function change at the thicker layers is a lack of order within these layers.

2. H_2O on Ru(001)

H_2O adsorbs on Ru(001) in a bilayer structure.[7] The exact nature of the two TPD peaks A_2 and A_1 associated with the first bilayer is still in debate.[7,8,16–18] Above one bilayer water grows as amorphous solid water [(ASW) at a temperature below 140 K], which desorbs at 162 K [Fig. 1(a), dashed line]. This peak slowly shifts to higher temperatures as coverage increases, typical to zero-order desorption kinetics. $\Delta\phi$ measurements during adsorption reveal a gradual decrease of 1.5 eV [Fig. 1(b), dashed line]. Most of the change in work function is due to the first bilayer (1.33 eV), while the rest is attributed to ASW layers. The slope of $\Delta\phi$ versus coverage is rapidly decreasing already at very low coverages. Since the sticking probability of water is close to unity and does not change with coverage, this change of slope has to be associated with structural changes that lead to a decrease of the effective dipole of absorbed water molecules. These changes were discussed in terms of water cluster formation upon adsorption at 82 K, by employing the kinetic model,[8] as well as molecular dynamics simulations.[19] A recent Fourier-transformed infrared (FTIR) study of this system suggested that indeed the first water layer grows initially via clusters formation.[20]

B. H_2O adsorption on top of CD_3Cl/Ru(001): $\theta_{H_2O} < 1$ BL, compression

Figure 2 shows a set of TPD spectra following the coadsorption of H_2O and CD_3Cl. Here 0.7 (monolayer) ML

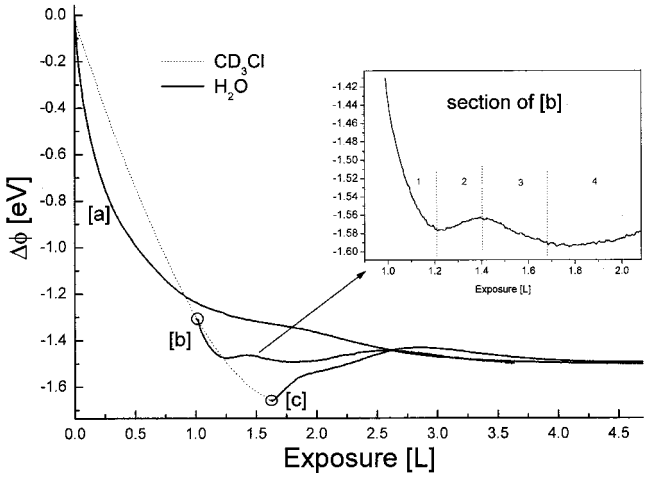

FIG. 3. Work function change measurement during adsorption of CD_3Cl followed by H_2O deposition. The initial $\Delta\phi$ response to CD_3Cl exposure is indicated as a dotted line [initial CD_3Cl coverages of 0.7 (b) and 1.1 ML (c)]. The subsequent work function change due to water deposition is shown as solid line. The inset reveals the case of water adsorption on top of 0.7 ML CD_3Cl. The final $\Delta\phi$ is practically identical in all cases.

CD_3Cl were deposited first at 82 K, and then increasing coverages of water were added on top. (In a previous work by Maschhoff *et al.*[9] the adsorption order was reversed, resulting in a completely different behavior.) The CD_3Cl TPD signal shows a complex dependence on water coverage, but the total uptake of the methyl chloride remains constant within 10%, as determined by integrating the area under the TPD peaks. Water molecules repel the CD_3Cl coadsorbates out of their normal adsorption sites, squeezing them into a gradually more densely packed phase. At the same time, H_2O TPD spectra remain practically unchanged compared to those of H_2O from Ru(001) in the absence of methyl chloride.

Up to water coverage of 0.44 bilayer (BL), the CD_3Cl TPD signal has significantly shifted from a broad peak in the range 150–200 K down to a narrower peak between 110 and 160 K. This is a result of dipole–dipole repulsion caused by the neighbor water molecules. The peak observed at 130–140 K is characteristic of CD_3Cl desorption from the second layer on the clean Ru(001). Adsorption of more than 0.44 BL of water on the same CD_3Cl coverage leads to a third, narrower TPD peak that emerges at 117 K, while the 150–160 K peak of the squeezed first layer is still there. The 117 K TPD peak appears at the same temperature as the third layer of clean methyl chloride molecules, or to CD_3Cl adsorbed on top of thick ASW layers [see dash-dotted line in Fig. 2(b)]. At higher water coverages up to 1 BL, practically all the CD_3Cl molecules desorb within a single narrow peak at 117 K.

More information on structural modifications within the adsorbed layers of CD_3Cl, as a result of water coadsorption, is obtained by monitoring work function change ($\Delta\phi$) during water adsorption. This is shown in Fig. 3. Water deposition on top of 0.7 ML [Fig. 3(b)] and 1.1 ML [Fig. 3(c)] of CD_3Cl results in oscillatory behavior of the work function change. This is best demonstrated for initial CD_3Cl coverage of 0.7 ML, as magnified in the inset to Fig. 3. Another important observation is that the asymptotic change in work function coincides with that of pure water adsorption on clean Ru(001) [Fig. 3(a)], regardless of the initial methyl chloride coverage.

The observed $\Delta\phi$ spectra can be explained as follows: Water adsorbs via cluster formation[8,20] as if there are no coadsorbed methyl chloride molecules. The growing clusters force the CD_3Cl molecules at submonolayer coverage to compress into islands of increasing density. This gradual compression leads to structural rearrangements inside the methyl chloride clusters that mimic the clean CD_3Cl adsorption behavior (opposite molecular orientation at the first and second layers) at far higher coverages. The TPD results suggest that a layered structure has been formed with three peaks at the expected temperatures for the first three layers. The $\Delta\phi$ data (see inset of Fig. 3) indicate that each of the TPD peaks (see Fig. 2, 0.44 BL of water) can be assigned to a corresponding work function change, displaying alternating orientation (on average) in each of the layers within the compressed molecules inside the three-dimensional (3D) islands. Similar behavior was observed in the adsorption of clean CD_3Cl (see Fig. 1).

The inset of Fig. 3 displays a $\Delta\phi$ curve obtained after adsorption of 0.7 BL CD_3Cl (1.0 L exposure), followed by water adsorption. In section 1 of this inset, adsorption of 0.2 L of water (0.2 L water are added to 1.0 L of preadsorbed CD_3Cl in the abscissa) leads to a further work function *decrease* of 170 meV. This value is a smaller decrease than that caused by the same amount of water on the clean metal (670 meV). This difference can be explained by the relocation of CD_3Cl from the first layer (broad peak at high temperatures, negative effect on the work function) to the second layer (desorption at 140 K, $\Delta\phi>0$).

In section 2, an *increase* of work function by 12 meV is the result of a combination of further compression and transfer of CD_3Cl from first (negative contribution to $\Delta\phi$) to second layer (positive contribution to $\Delta\phi$). This effect combines with the negative contribution of further water adsorption of about 250 meV (still less than its contribution in section 1). Here, where the negative contribution of water molecules is reduced, flipping of the CD_3Cl molecules becomes the dominant effect, resulting in the actual switch of the work function from negative to positive change. In section 3, the water coverage increases to 0.7 BL and a decrease of 27 meV in the work function is recorded. In this coverage range TPD shows the onset of population of the third layer of CD_3Cl (peak desorption at 117 K) as a result of the increased compression by the water molecules. An increase in the number of third layer molecules [$\Delta\phi<0$, see Fig. 1(b)], while decreasing second layer population ($\Delta\phi>0$) in addition to further water adsorption ($\Delta\phi<0$) necessarily results in a net decrease of the work function.

To conclude, at least three layers of CD_3Cl are formed within 3D molecular islands upon water post-adsorption. This is evidenced by both ΔP-TPD and $\Delta\phi$ data, when 0.7 ML of methyl chloride is predeposited. Other CD_3Cl initial

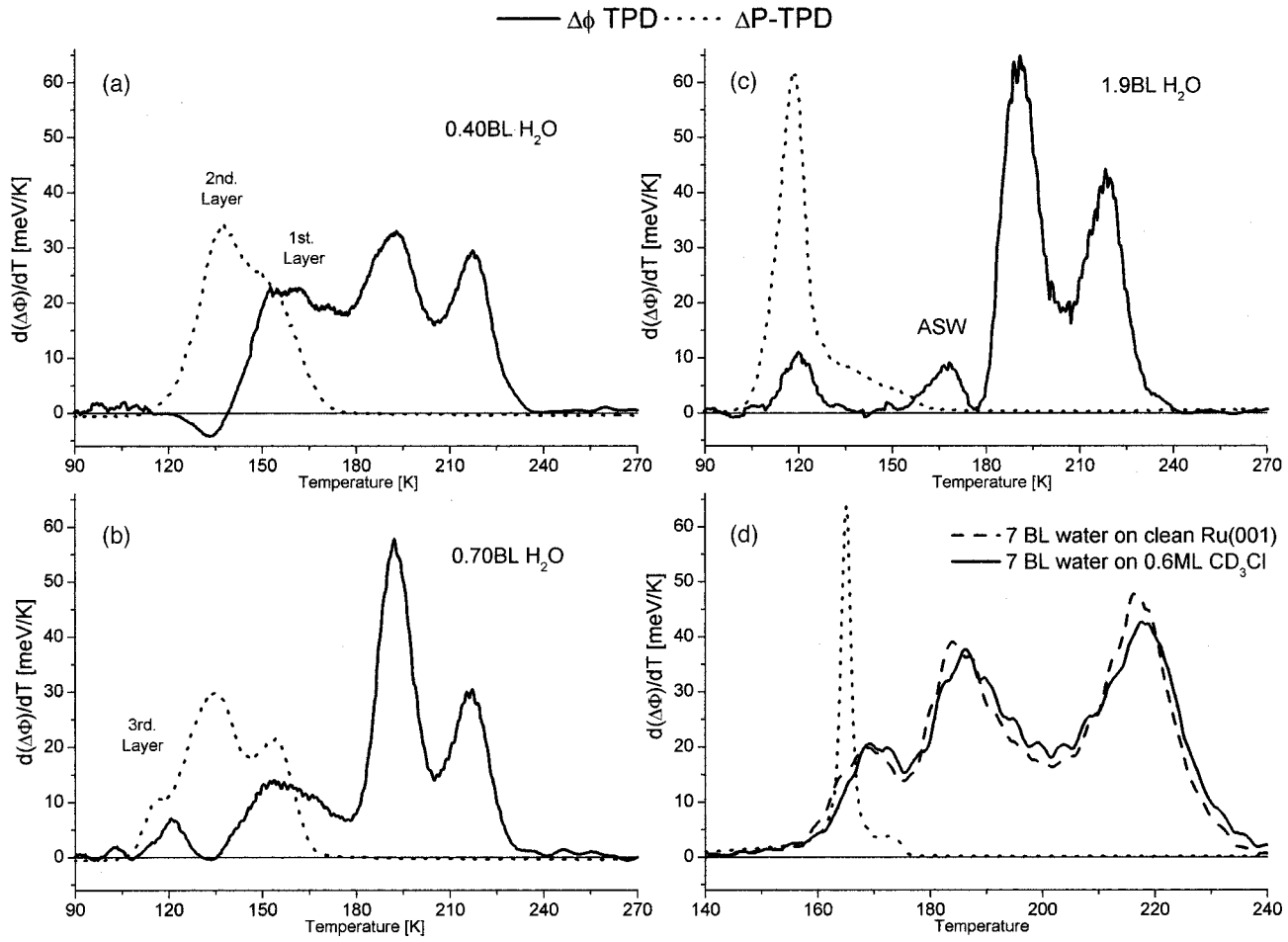

FIG. 4. Comparison between ΔP-TPD (CD_3Cl, dotted line) and $d(\Delta\phi)/dT$ (solid line) for the indicated water coverages on top of preadsorbed 0.7 ML CD_3Cl. The $\Delta\phi$-TPD peaks at 195 and 215 K are the work function response to H_2O desorption. (d) shows a comparison between $d(\Delta\phi)/dT$ of clean H_2O (dashed line) and H_2O caging CD_3Cl (solid line). Note that there is practically no $\Delta\phi$ response to the desorption of caged CD_3Cl (see text for discussion).

coverages undergo the same compression process, but reveal more complex behavior. As a result, it is more difficult to resolve the changes in $\Delta\phi$.

Moreover, at higher water coverages, an asymptotic work function change value of pure water is obtained, independent of the methyl chloride coverage. This observation indicates that at high water coverage, water molecules penetrate underneath the methyl chloride clusters, avoiding any direct contact of these molecules with the metal surface. The desorbing CD_3Cl molecules do not affect the measured work function change under these conditions. This penetration effect under the methyl chloride layer starts already at water coverage of about 1 BL, as revealed from the significant change in the TPD spectrum, shown in Fig. 2, 0.98 BL of water. This spectrum is practically identical to that observed after adsorbing CD_3Cl on top of initially adsorbed 5.3 BL of water [dash-dotted line in Fig. 2(b)].

Evidence for orientation changes within the compressed three layers of CD_3Cl is obtained also from differentiation of the $\Delta\phi$-TPD spectra. By plotting $d(\Delta\phi)/dT$ versus temperature, one can resolve the individual TPD peaks according to their contribution to the work function. Three such plots are shown for different water coverages on top of 0.7 ML CD_3Cl in Figs. 4(a)–4(c). The signal is a combination of the contributions of both CD_3Cl and H_2O during their respective desorptions. In order to distinguish between these different contributions, the ΔP-TPD signal of CD_3Cl is plotted (dotted line) while the corresponding water coverage is indicated. The ΔP-TPD spectrum is normalized to adjust its scale with that of the $d(\Delta\phi)/dT$ plot. After adsorption of 0.4 BL water on top of the 0.7 ML CD_3Cl, two water peaks appear at 216 and 192 K in the $d(\Delta\phi)/dT$ spectrum. The broad peak in the range 150–170 K ($\Delta\phi>0$) and the small opposite peak at 135 K ($\Delta\phi<0$) are attributed to the first and second compressed layers of CD_3Cl, respectively. At 0.7 BL water coverage, the contribution of the first layer is significantly reduced, while a peak at 120 K ($\Delta\phi>0$) appears. As discussed above, molecules in the third layer are indeed expected to lead to a positive contribution to $\Delta\phi$. At higher water coverages (1.9 BL in Fig. 4) the contribution to the total $\Delta\phi$ due to ASW appears at 165 K, while the sole contribution from CD_3Cl desorption is at 120 K. There are no traces of CD_3Cl molecules desorbing from "typical" first or second layers. It is concluded that at water coverages above 1 BL, the 3D methyl chloride islands become rather disordered and therefore do not affect the measured work function change.

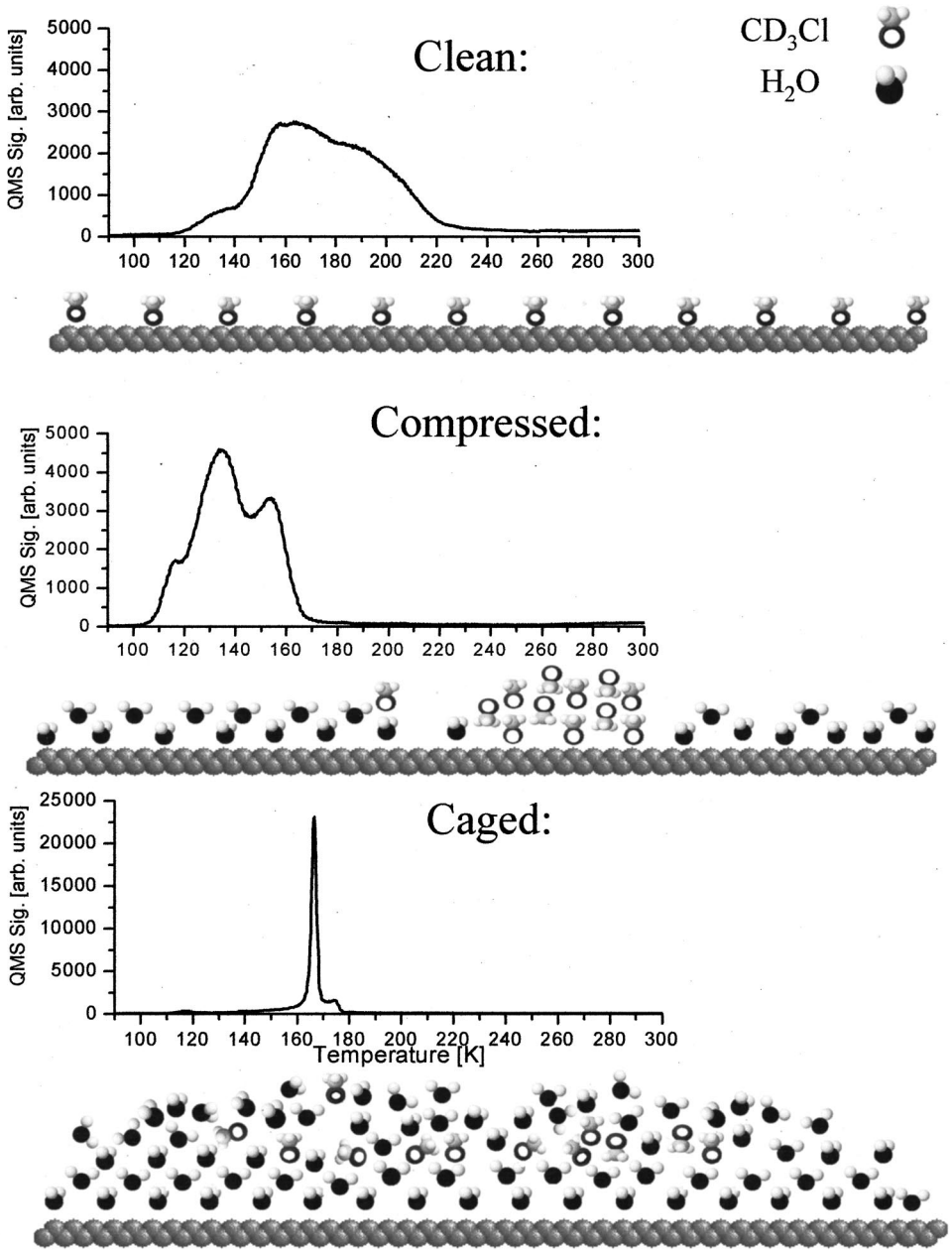

FIG. 5. CD_3Cl/H_2O coadsorption system. The CD_3Cl layer is initially compressed into 3D islands. The methyl chloride molecules are eventually encapsulated and caged within the water hydrogen-banded network.

C. H_2O adsorption on top of CD_3Cl/Ru(001): $\theta_{H_2O} > 1$ BL, caging

At water coverages above 2.2 BL (Fig. 2), desorption of CD_3Cl shifts from 120 to 115 K and at the same time a new broad peak appears at 160 K. The peak at 115 K is identical to a TPD peak obtained following a reversed adsorption order: post-adsorption of CD_3Cl *on top* of 7 BL of water, superimposed as a dash-dotted line in Fig. 2(b), 5.3 BL of water. At coverages of 3 BL and above a very sharp new peak emerges at 160 K. Further increase of the water coverage results in three trends: (a) The peaks at 115 and 150 K gradually vanish. (b) The peak at 160 K slowly moves to higher temperature (up to 165 K), while becoming increasingly narrow in an explosive desorption mode. The caged methyl chloride molecules eventually desorb within a peak width of 2 K. (c) A new desorption shoulder appears at 172 K.

A sharp ''explosive'' TPD peak of molecules that are trapped under layers of water is indicative of cage formation. This phenomenon was reported for the first time by Livneh *et al.* in the case of N_2 molecules covered by water on Ru(001).[11] The CD_3Cl molecules can desorb only after the onset of water desorption, as shown in Fig. 4(d). The CD_3Cl desorption temperature under water-cage conditions was earlier attributed for the case of CCl_4 to the phase transition temperature of ASW to crystalline ice.[12] This phase transition could be recorded as a change in the slope of the water TPD peak at the crystallization temperature.[12] The small CD_3Cl peak observed at higher temperature (172 K in Fig. 2, 10 BL of water: this peak contains 15% of the total peak area) follows precisely the desorption peak of bulk ice. This codesorption suggests that about 15% of the CD_3Cl molecules are dissolved within the bulk crystalline ice and codesorb with it.

Figure 4(d) demonstrates, by means of comparative $d(\Delta\phi)/dT$ plots, the absence of any influence of caged CD_3Cl on the measured $\Delta\phi$-TPD spectrum. Adsorption of 0.7 ML of CD_3Cl on clean Ru(001) decreases the work function by 1.3 eV. When this amount of CD_3Cl is caged under thick water layers, the resulting $d(\Delta\phi)/dT$ spectra are identical to those obtained when only water is adsorbed on Ru(001). This suggests that the caged molecules are not in direct contact with the metal surface.

Moreover, the dipoles of the encapsulated, layered molecules seem to cancel each other, indicating a high degree of disorder. This observation is supported by the asymptotic $\Delta\phi$ values obtained upon adsorption of high water coverage, as discussed above: see Fig. 3.

We take the liberty to speculate that the unique encapsulation or caging phenomenon of molecules inside amorphous solid water, and in particular those that display hydrophobic interactions, like methyl halides, resemble clathrate hydrates.[21,22]

These unique water cages that form under pressure at the bottom of oceans are thought to keep vast amounts of methane and possibly other hydrocarbons. The low-temperature, high-density mechanism of encapsulation that occurs rather generally on solid surfaces, as described above, may suggest a clue for the mechanism of clathrate hydrates formation.[21–23]

IV. CONCLUSIONS

Adsorption of water on top of CD_3Cl shows two major trends, as summarized in Fig. 5. At submonolayer coverage of methyl chloride and low post-adsorbed water coverage, methyl chloride molecules are being compressed by water into high-density 3D islands. This is indicated by CD_3Cl TPD peaks that are shifted to lower temperatures and are accompanied by characteristic, distinct CD_3Cl layers. Water coverages of more than 1 BL lead to full detachment of the methyl chloride molecules from the ruthenium surface, to become encapsulated within the amorphous solid water layer that is formed. At even higher water coverage, the methyl chloride TPD peak temperature rises to 165 K, indicating that the CD_3Cl is gradually caged within the ASW layers.

This caging effect is a general phenomenon that has been demonstrated already for several different molecules, e.g., N_2, CCl_4, CO_2, and O_2. Unlike the previous systems, in the case of methyl halides with their permanent and relatively large dipole moment, 3D clusters are formed during the first stage of water adsorption, up to 1 BL. At higher coverages, the methyl chloride molecules are pushed away from the surface, to be encapsulated and caged within the amorphous solid water layer, disordered enough to have no effect on the measured work function change during TPD.

ACKNOWLEDGMENTS

This work was partially supported by a grant from the Israel Science Foundation and the U.S. Israel Binational Science Foundation.

[1] E. V. Albano, J. Chem. Phys. **85**, 1044 (1985).
[2] *Physics and Chemistry of Alkali Metals Adsorption*, edited by H. P. Bonzel, A. M. Bradshaw, and G. Ertl (Elsevier, Amsterdam, 1989).
[3] (a) R. W. Verhoef, W. Zhao, and M. Asscher, J. Chem. Phys. **106**, 9353 (1997); (b) J. Neugebauer and M. Scheffler, Phys. Rev. Lett. **71**, 577 (1993); (c) R. W. Verhoef and M. Asscher, Surf. Sci. **376**, 389 (1997).
[4] A. Berko, W. Erley, and D. Sander, J. Chem. Phys. **93**, 8300 (1990).
[5] B. L. Maschhoff and J. P. Cowin, J. Chem. Phys. **101**, 8138 (1994).
[6] T. Livneh, Y. Lilach, and M. Asscher, J. Chem. Phys. **111**, 11 138 (1999).
[7] P. A. Thiel and T. E. Madey, Surf. Sci. Rep. **17**, 211 (1987); M. A. Henderson, *ibid.* **46**, 1 (2002).
[8] Y. Lilach, L. Romm, T. Livneh, and M. Asscher, J. Phys. Chem. B **105**, 2736 (2001).
[9] B. L. Maschhoff, M. J. Lemeda, M. Kwini, and J. P. Cowin, Surf. Sci. **359**, 253 (1996).
[10] S. K. Jo and J. M. White, Surf. Sci. **255**, 321 (1991).
[11] T. Livneh, L. Romm, and M. Asscher, Surf. Sci. **315**, 250 (1996).
[12] R. S. Smith, C. Huang, E. K. L. Wong, and B. D. Kay, Phys. Rev. Lett. **79**, 909 (1997).
[13] C. L. Perkins and M. A. Henderson, J. Phys. Chem. B **105**, 3856 (2001).
[14] T. Livneh and M. Asscher, Langmuir **14**, 1348 (1998).
[15] T. Kawaguchi, M. Hijikigawa, Y. Hayafuji, M. Ikeda, R. Fukushima, and Y. Tomiie, Bull. Chem. Soc. Jpn. **46**, 53 (1973).
[16] G. Held and D. Menzel, Surf. Sci. **316**, 92 (1994).
[17] G. Held and D. Menzel, Phys. Rev. Lett. **74**, 4221 (1995).
[18] G. Pirug, C. Ritke, and H. P. Bonzel, Surf. Sci. **241**, 289 (1991).
[19] Y. Lilach and M. Asscher (unpublished).
[20] M. Nakamura and M. Ito, Chem. Phys. Lett. **325**, 293 (2000).
[21] J. A. Ripmeester, C. I. Ratcliffe, J. S. Tse, and B. M. Powell, Nature (London) **325**, 135 (1987).
[22] T. Head-Gordon, Proc. Natl. Acad. Sci. U.S.A. **92**, 8308 (1995).
[23] K. A. Udachin and J. A. Ripmeester, Nature (London) **397**, 420 (1999).